2006

Powerful High-Velocity Dispersion Molecular Hydrogen Associated with an Intergalactic Shock Wave in Stephan's Quintet

PN Appleton

KC Xu

W Reach

MA Dopita

Y Gao

See next page for additional authors

Authors

PN Appleton, KC Xu, W Reach, MA Dopita, Y Gao, N Lu, CC Popescu, JW Sulentic, RJ Tuffs, and Min Yun

Powerful High Velocity-dispersion Molecular Hydrogen associated with an Intergalactic Shock Wave in Stephan's Quintet

P. N. Appleton[1], Kevin C. Xu[2], William Reach[1], Michael A. Dopita[3], Y. Gao[4], N. Lu[1], C. C. Popescu[5], J. W. Sulentic[6], R. J. Tuffs[5] AND M. S. Yun[7]

[1]Spitzer Science Center, California Institute of Technology, 1200 E. California Blvd., Pasadena CA 91125

[2]IPAC, California Institute of Technology, 1200 E. California Blvd., Pasadena CA 91125

[3]Research School of Astronomy and Astrophysics, The Australian National University, Cotter Road, Weston Creek, ACT 2611, Australia

[4]Purple Mountain Observatory, Chinese Academy of Sciences, 2 West Beijing Road, Nanjing 210008, China

[5]Max Planck Institute für Kernphysik, Saupfercheckweg 1, 69117 Heidelberg, Germany

[6]Department of Physics and Astronomy, University of Alabama, Tuscaloosa, AL 35487

[7]Department of Astronomy, University of Massachusetts, Amherst, MA 01003

ABSTRACT

We present the discovery of strong mid-infrared emission lines of molecular hydrogen of apparently high velocity dispersion ($\sim$870 km s^{-1}) originating from a group-wide shock wave in Stephans Quintet. These *Spitzer Space Telescope* observations reveal emission lines of molecular hydrogen and little else. This is the first time an almost pure H_2 line spectrum has been seen in an extragalactic object. Along with the absence of PAH-dust features and very low excitation ionized gas tracers, the spectra resemble shocked gas seen in Galactic supernova remnants, but on a vast scale. The molecular emission extends over 24 kpc along the X-ray emitting shock-front, but has ten times the surface luminosity as the soft X-rays, and about one-third the surface luminosity of the IR continuum. We suggest that the powerful H_2 emission is generated by the shock wave caused when a high-velocity intruder galaxy collides with filaments of gas in the galaxy group. Our observations suggest a close connection between galaxy-scale shock waves and strong broad H_2 emission lines, like those seen in the spectra of Ultraluminous Infrared Galaxies where high-speed collisions between galaxy disks are common.

Subject headings: galaxies: interactions, intergalactic medium, individual (NGC 7318b), evolution.

1. Introduction

Stephan's Quintet (hereafter SQ) is a system of four strongly interacting galaxies in a compact group, and a likely foreground galaxy seen in projection against them (Allen 1970). One of the most remarkable aspects of SQ is a $\sim$40 kpc long non-thermal radio continuum structure (see Fig.1) lying in intergalactic space between the galaxies (Allen & Hartsuiker 1972; van der Hulst 1981). The same structure is also seen in X-rays, and has been shown to be consistent with a large-scale shock wave, based on the optical spectroscopy (Pietsch et al. 1997; Trinchieri et al. 2005; Xu et al. 2003). It is probable (Sulentic et al. 2001) that the shock wave has formed because a high-velocity "intruder" galaxy, NGC 7318b, is colliding with the inter-group-medium (IGM) located within the main group. We assume here a group distance of 94 Mpc, assuming a Hubble constant of 70 km s^{-1} Mpc^{-2} and a systemic velocity for the group as a whole of 6600 km s^{-1}.

2. Observations

We used the Infrared Spectrograph (Houck et al. 2004) on board the *Spitzer Space Telescope*[1] to take mid-IR spectra at the peak in the IR/radio emission from the shocked region. Observations were made on November 17 and

---

[1]This work is based on observations made with the *Spitzer Space telescope* which is operated by the Jet Propulsion Laboratory, California Institute of Technology, under NASA contract 1407.
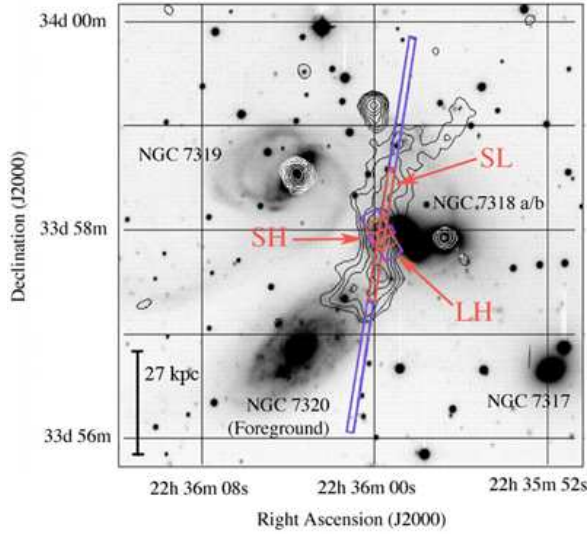
Fig.1 Stephan's Quintet showing the positioning of the IRS slits centered on α(J2000) = 22h 35m 59.57s, δ(J2000) = +33d 58m 1.8s. Contours are VLA 1.4 GHz radio emission superimposed on an R-band optical image(Xu et al. 2003). The X-ray emission (not shown here) follows closely that of the radio. Only the central portion of the slits (red boxes) were common to the two separate observing (nod) positions made in each IRS module slit (the purple shows the full coverage). Short-Low = SL = 57 x 3.6 arcsecs^2, Short-High = SH = 11.3 x 4.7 arcsec^2, and Long-High = LH = 22.3 x 11.1 arcsecs^2. The scale bar assumes a distance to the group of 94 Mpc.

December 8 2004 using the Short-Low (SL), Short-Hi (SH) and Long-Hi (LH) modules of the spectrograph covering the wavelength range λ5.3-14.0μm, λ10.0-19.5μm and λ18.8-37.2μm respectively. The raw data were processed through the SSC IRS S11-science pipeline to create 2-d flat-fielded images of the spectral orders. These data were further processed to remove the effects of the so-called rogue pixels which were not corrected by the pipeline. These pixels have erratic high dark-currents which vary with time, and were replaced using a simple pixel interpolation scheme. Flux and wavelength calibration was performed using the standard calibration methods (Decin et al. 2004). Final extraction of the 1-d spectra was made using the SSC software SPICE, and line fluxes were measured using SMART.
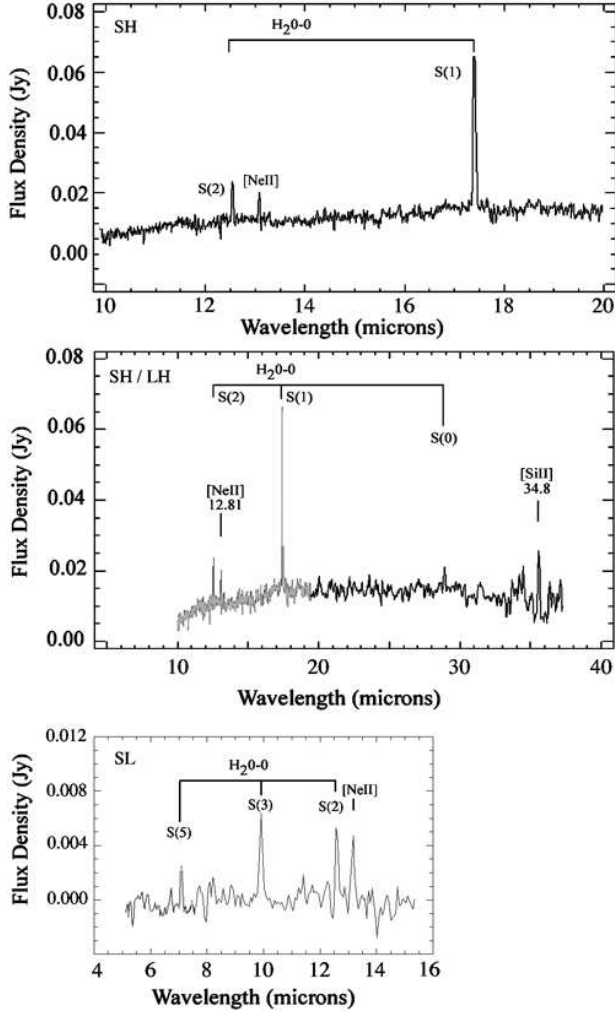
Fig.2 a) The IRS SH spectrum of the brightest radio/IR point in the shock-front. b) the combined SH (grey) and LH (black) spectrum of the same target region assuming that the continuum can be used to match the two spectra at 20μm, and c) the SL spectrum at the same position. The SL2 (grey) and SL1 (black). Note that there is no evidence for PAH emission.

3.   Results

Figure 2a, b and c show the spectra extracted in the region where all three slits overlap. Except for the atomic lines of [NeII]λ12.8μm and [SiII]λ34.8μm, all are rotational transitions of the ground vibrational states of molecular hydrogen (the 0-0 S(0), S(1), S(2),

S(3) and S(5) lines). To explore the excitation of the observed H_2 gas we need to compare the line fluxes from the IRS slits which have different projected sizes on the sky: requiring that we make some assumptions about the spatial distribution of the molecules over the scale of the slits. From the SL slit oriented along the shock structure, we found that the H_2 emission was extended on the scale of 52 arcsecs (24 kpc), declining slowly from a small peak at the pointing centre. We therefore consider three possible distributions: a) the H_2 originates in a point source–an unrealistic limiting case, b) the H_2 is extended with constant surface brightness over the slits, and c) a "preferred" case based on the observed SL distribution, assuming it has a similar spatial width to the radio emission. Table 1 provides a list of the lines and their measured fluxes, including upper limits for some key undetected lines.

Figure 3 shows the excitation diagram for H_2, (N/g) versus the upper-level energy, for the 5 detected and one undetected hydrogen transitions. N is the molecular column density, g is the statistical weight for that transition. The non-linear decline of log (N/g) with upper-level energy is commonly seen in shocks within the Galaxy, as well as in external galaxies (Lutz et al. 2003; Rigopoulou et al. 2002), and is an indication that no single temperature LTE model fits these data. There are no obvious deviations from the assumed ortho/para ratio = 3 visible in these plots. We fit a multi-temperature model through the "preferred" data points, constraining the warm gas by the S(0)/S(2) [para] ratio, and allowing the higher order S(3)/S(5) [ortho] transitions to provide a very rough guide to the temperature of a hotter component. Our data are consistent with a warm T = 185±30K component (H_2 column density 2.06 × 10^{20} cm^{-2}) and T = 675±80K (column 1.54 × 10^{18} cm^{-2}) for the hotter components. The choice of a 2-component temperature model (especially the hotter component) is quite arbitrary: in reality (if our interpretation is correct that the emission arises in a highly turbulent medium) it is likely to be the sum of a continuous distribution of multi-temperature components. However, the coolest component

dominates the hydrogen column density estimates given here. We note that a multi-phase medium could also lead to a similar excitation pattern.
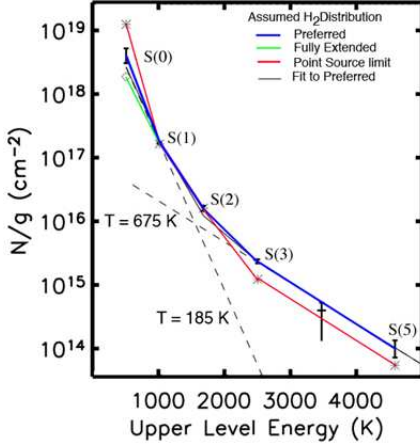
The excitation diagram for H_2. The colored lines represent three different assumed spatial distributions of the H_2 across the LH and SH slits. For SL, we scale the spectrum to that of SH using the 0-0 S(2) line which is detected in common. The blue line (and error bars) represents the "preferred" distribution based on an extrapolation from the H_2 distribution seen in the SL slit (see text), the green line and red show the limiting cases of an infinite and point source distribution respectively. The dotted lines represent a rough model for the "preferred" distribution which assumes a two-temperature fit to the points. The solid line represents the sum of these components.

The total H_2 line luminosity, accounting for an extra 40% in undetected lines, is 8.4×10^{40} ergs s^{-1} from the SH slit area alone. The corresponding H_2 mass in these warm/hot components seen in the SH slit is 3.4×10^7 M$_\odot$ ($\Sigma_{H_2} = 3.1$ M$_\odot$ pc^{-2}). The H_2 surface luminosity of 2.0 L$_\odot$ pc^{-2}, is only a factor of three less than the IR continuum surface luminosity of 5.4 L$_\odot$ pc^{-2} (= 2.5×10^{41} ergs s^{-1}) based on an extrapolation from unpublished 70μm Spitzer data by one of us (RJT–and consistent with earlier ISO data from Xu et al. 2003). The corresponding H_2 lines and FIR continuum surface brightnesses are 10$\times$ and 26$\times$ the X-ray (0.5–1.5 kev) surface brightness (0.21 L$_\odot$ pc^{-2}) respectively. The dominance of the FIR continuum emission over the X-ray emission confirms that the shocked gas is cooling primarily through inelastic collisions of the ions and electrons with

grains, as proposed by (Xu et al. 2003–who derived a cooling timescale of $\sim$2 Myrs), and may explain the unexpectedly cool post-shock X-ray gas seen in recent XMM observations (Trinchieri et al. 2005). However, the fact that a substantial minority of the total cooling also proceeds through H_2 lines comes as a surprise.

A remarkable feature of the Spitzer observations (Fig.4) is the discovery that the H_2 line is extremely broad and resolved spectrally, even with the relative low resolution of the IRS (R=600). Assuming a Gaussian decomposition from the instrument profile, we estimate the intrinsic width of the 0-0 S(1) line to be 870 $\pm$60 km s^{-1}: exceeding the largest known H_2 line-width known to date (e. g. the ULIRG NGC 6240; ΔV $\sim$ 680 km s^{-1}) (Lutz et al. 2003; Armus et al. 2005). Because H_2 is a fragile molecule which can easily be destroyed in 50 km s^{-1} J-shocks (Hollenbach & McKee 1980; Hollenbach & McKee 1989), such a wide, potentially intrinsic, spread in molecular cloud velocities is extremely unusual.

The line-width is comparable with the collision-velocity (ΔV $\sim$500-600 km s^{-1}) of NGC 7318b with either NGC 7319 or an inter-galactic gas filament (Allen & Hartsuiker 1972; van der Hulst 1981; Williams et al. 2002; Sulentic et al. 2001; Trinchieri et al. 2003; Trinchieri et al. 2005), suggesting that the H_2 emission is intimately linked to the formation of the radio and X-ray shock structure.
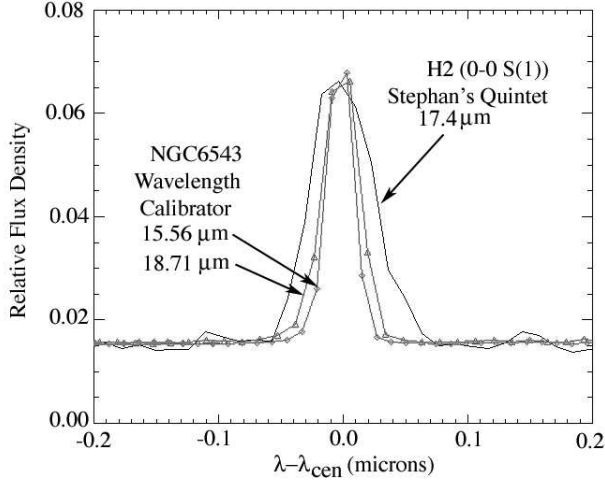
Fig.4 The 0-0 S(1)17.0μm molecular hydrogen line (detected with a signal to noise ratio of 33) is clearly resolved (intrinsic FWHM = 870±60 km s^{-1}) by the IRS (black) as compared with two unresolved spectral lines (R = 600) in the planetary nebula NGC 6543 at 15.6 and 18.7μm which bracket the H$_2$ line (grey). Similar broad widths are found for the 0-0 S(0) and 0-0 S(2) lines. The width of the [NeII]λ12.8μm line is significantly less broad (intrinsic FWHM = 600±80 km s^{-1}). λ_{cen} is the wavelength of the line center for the three lines shown in order to allow their widths to be compared.

Although the IRS does not have the spectral resolution to determine whether the apparently broad line is made up of a number of narrow line components blended together along the line of sight, or whether the line is truly broad, there are some pieces of evidence that favor the latter. These are, 1) broad ($\Delta V = 1000$ km s^{-1}) optical [OI]λ6300 line emission with excitation properties of shocked gas is seen at our observing position (Xu et al. 2003), whereas at other positions much further from the peak of the X-ray/IR ridge narrower lines are seen, (2) Extremely high speed shocks are highly dissociative, and it is unlikely that pre-existing H$_2$, nor even more fragile PAH molecules, could survive a >500 km s^{-1} collision with the intruder (Hollenbach & McKee 1980; Hollenbach & McKee 1989). Furthermore, the H$_2$ line luminosity we see from the region ($\sim$2 L$_\odot$ pc^{-2}) is a significant fraction of the predicted (Dopita & Sutherland 1995; Dopita & Sutherland 1996) mechanical luminosity

density in the shock ($160 \times$ the Hα surface density, $\sigma_{H\alpha} = 160$ x 0.13 L$_\odot$ pc^{-2} = 21 L$_\odot$ pc^{-2}). There would appear to be plenty of mechanical luminosity available to excite the H$_2$ molecules if they reformed in post-shocked gas.

If we assume a 500 km s^{-1} shock is driven into the IGM, and second similar shock into the intruder (assuming their densities are similar), this will create an unstable turbulent ($\Delta V \sim 1000$ km s^{-1}) cooling layer where the flows mix. If the gas can cool quickly enough, H$_2$ recombination would occur in that layer, and this would have the necessary properties to explain our observations–including the high velocity dispersion from turbulence. The cooling timescale (Dopita & Sutherland 2003) for the hot X-ray gas in each shock wave, τ_{cool} (Myrs) = 0.24 $(V_{500})^{4.4}/Zn$, where V_{500} is the speed of the shock in units of 500 km s^{-1}, Z is the metallicity in solar units and n is the pre-shock density (we assume $n = 0.027$ cm^{-3} , from X-ray observations (Trinchieri et al. 2003)). For $V_{500} \sim 1$, $Z = 1$, $\tau_{cool} = 9.5$ Myrs, during which time the shock wave would have travelled ~ 5kpc = 10 arcsecs (or twice this for the double shock). In reality, the cooling layer would be much sharper, since this analysis excludes the effects of IR-cooling by dust which is known to be very significant (Xu et al. 2003). This argument demonstrates that the post-shocked gas layer would cool fast enough to begin forming H$_2$ within the viewing zone of the IRS slits even for a mainly transverse geometry for the shock propagation as projected on the sky, The observed H$_2$ column of the cooler component ($\sim 2 \times 10^{20}$ cm^{-3}) could easily be built up over a scale of a few kpc from the available pre-shocked gas mass once the temperature of the gas had cooled sufficiently for H$_2$ to form.

One challenge for the post-shock origin of the H$_2$ is to avoid putting too much of the shock dissipation energy into the X-ray component. Usually in high-speed shocks, X-ray dissipation dominates the cooling in the T= 10^6 to 10^4 K regime, before H$_2$ molecules can form: not the case here since H$_2$ line emission exceeds the X-rays by a factor of ten. Part

of the answer may come from the even stronger IR continuum seen at longer wavelengths (Xu et al 2003). These authors argued that the principal coolant in the shock is from large grains which efficiently cool the shock through far-IR emission. The H_2 emission from the post-shocked material could be additionally boosted relative to the X-rays by invoking a glancing collision between the intruder galaxy and the IGM–which would create an oblique-shock geometry rather than a plane-parallel one. In oblique shocks, much more energy is carried in bulk transverse motions (hence reducing X-ray dissipation), and the shock is significantly weakened (e. g. Dopita 2003), while still allowing a fraction of the mechanical energy to cascade down to smaller and smaller scales (as in the Galactic ISM e. g. McKee, Chernoff & Hollenbach 1984; Elmegreen & Scalo 2004), where shock-speeds would be lower and molecules could re-form in the post-shocked medium. To test these ideas will require detailed 3-d hydrodynamic models beyond the scope of this observational paper.

An alternative explanation for the H_2 emission is to postulate that the emission comes from a 500 km/s shock overrunning a clumpy pre-shocked medium. This has the advantage that dense clouds (embedded in a more diffuse medium) will experience much slower shocks and are more likely to cool through line emission than X-rays, whereas the FIR emission could come from grains emitting over the entire diffuse medium–thus partly explaining the anomalous H_2 line to IR continuum ratio. The large velocity dispersion could arise because the shock would eventually accelerate clouds to different velocities within the shock, or because of multiple velocity components being present in the pre-shocked gas. The problem with this picture is that we might expect to see PAH emission from the precursor ISM which is not observed. We note that if the $H\alpha$ emission seen from the shocked regions was scaled to an equivalent PAH line strength typical of those seen in the largest of the M51 HII regions (Calzetti et al. 2005), we should have easily (>10-sigma) detected the signal even in the case of no extinction correction for the $H\alpha$. Of course the ISM of any

precursor material is likely to contribute only a small factor to the Hα emission observed, but this provides an upper limit. The shock is also likely to be radiative, which could also help to destroy PAH molecules, whereas the more refactory grains must have been able to survive the shock. This model still has to be capable of predicting the large ratio of H$_2$ line luminosity relative to the IR continuum luminosity–implying a lot of energy has to be somehow channeled into mechanical energy. Further modeling of these scenario will be required in order to determine whether it can explain all the available data on the shock.

Future H$_2$ observations with much higher velocity and spatial resolution may allow us to explore further the nature of the emission mechanism that is generating such large H$_2$ line flux. There are hints of large-scale clumpyness in the H$_2$ distribution as seen by SL along the shock front, and studying the velocity and spatial inhomogenities within the shock would be highly beneficial.

4. Implications for ULIRGs

The discovery of strong, high velocity-dispersion H$_2$ emission in a large-scale group-wide shock wave provides support for the idea (Rieke et al. 1985), that shock waves are primarily responsible for the strong H$_2$ emission lines seen in many Ultraluminous Infrared Galaxies (ULIRGs). Indeed our observations suggest L(H$_2$) $> 10^{41}$ ergs s^{-1} over the whole shock structure–comparable to the H$_2$ luminosity of Arp 220, but a factor of ten less than NGC 6240 (Armus et al. 2005). An alternative idea for NGC 6240 is that X-rays heating the gas, rather than shocks, is the dominant mechanism for the IR lines in ULIRGs (Draine & Woods 1990). However, in addition to the low X-ray surface density compared with the H$_2$ lines, our spectra of SQ, show little evidence of the H$_3^+\lambda16.33\mu$m line: a key diagnostic of this model. Although the geometry of the shocks are unlikely to be identical to that suggested by the SQ observations, there is little doubt that large-scale shocks must

be present in ULIRGs, where high velocity streams of molecular gas must collide–especially in the early stages of a merger.

REFERENCES

Allen, R. J. 1970, A&A, 7,330

Allen, R. J. & Hartsuiker, J. W. 1972, Nature, 239, 324

Armus, L. et al. 2004, ApJS, 154, 178

Armus, L. et al. 2005, ApJ, submitted

Calzetti, D. et al. 2005, ApJ, 633, 871

Decin, L., Morris, P. W., Appleton, P. N., Charmandaris, V. & Houck, J. R. 2004, ApJS, 154, 408

Dopita, M. A. & Sutherland, R. S. 1995, ApJ455, 468 (1995)

Dopita, M. A. & Sutherland, R. S. 1996, ApJS, 102, 161 (1996)

Dopita. M. A. & Sutherland, R. S. 2003, Astrophysics of the Diffuse Universe, (Berlin: Springer-Verlag), p201

Draine, B. T. & Woods, D. T. 1990, ApJ363, 464

Elmegreen, B. G. & Scalo, J. 2004, ARAA, 42, 211

Hollenbach, D. & McKee, C. F. 1980, ApJ, 241, L47-L50

Hollenbach, D. & McKee, C. F. 1989, ApJ, 342, 306

Houck, J. R. et al. 2004, ApJS, 154, 18

Lutz, D., Sturm, E., Genzel, R., Spoon, H. W. W., Moorwood, A. F. M., Netzer, H. & Sternberg, A. 2003, A&A, 409, 867

McKee, C. F., Chernoff, D. F. & Hollenbach, D. J. 1984, Infrared spectroscopy of interstellar shocks, in Galactic and Extragalactic Infrared Spectroscopy: Proceedings of the Sixteenth ESLAB Symposium, (Dordrecht: Reidel)

Pietsch, W., Trinchieri, G., Arp, H. & Sulentic, J. W. 1997, A&A, 322, 89

Rieke, G. H., Cutri, R. M., Black, J. H., Kailey, W. F., McAlaray, C. W., Lebofsky, M. J. & Elston, R. 1985, ApJ, 290, 116

Rigopoulou, D., Kunze, D., Lutz., D.,Genzel, R. & Moorwood, A. F. M. 2002, A&A, 389, 374

Sulentic, J. W., Rosado, M., Dultzin-Hacyan, D., Verdes-Montenegro, L., Trinchieri, G., Xu, C. & Pietsch, W. 2001, AJ, 122, 2993

Trinchieri, G., Sulentic, J., Breitschwerdt, D. & Pietsch, W. 2003, A&A401, 173

Trinchieri, G., Sulentic, J., Pietsch, W. & Breitschwerdt, D. 2005, A&A, in press

van der Hulst, J. M. & Rots, A. H. 1981, AJ, 86, 1175

Williams, B. A., Yun, M. S. & Verdes-Montenegro, L. 2002, AJ, 123, 2417

Xu, K., Lu, N., Condon, J. J., Dopita, M. & Tuffs, R. J. 2003, ApJ, 595, 665

Table 1.   Line Fluxes Scaled to the Equivalent SH-slit Aperture

Spectral Feature	IRS Module	Flux $\times\ 10^{-22}$ W cm^{-2} (Uniform)[a]	Flux $\times\ 10^{-22}$ W cm^{-2} (Point Source Limit)[a]	Flux $\times\ 10^{-22}$ W cm^{-2} (Preferred)[a]
H_2 0-0 S(0)	Long High	1.9±0.5	12.6±3.3	4.2±1.1
H_2 0-0 S(1)	Short High	19.80±0.57	19.80±0.57	19.80±0.57
H_2 0-0 S(2)	Short High	6.41±0.58	6.41±0.58	6.41±d0.58
H_2 0-0 S(3)	Short Low	15.6±1.1	8.1±1.1	15.6±1.1
H_2 0-0 S(4)	Short Low	< 3.4±1.1	< 1.8±1.1	< 3.4±1.1
H_2 0-0 S(5)	Short Low	7.8±2.4	4.1±2.4	7.8±2.4
$[NeII]$12.81μm	Short High	3.49±0.64	3.49±0.64	3.49±0.64
$[NeIII]$15.55μm	Short High	<1.5±0.64[b]	<1.5±0.64[b]	<1.5 ±0.64[b]
$H_3{}^+$ 16.33μm	Short High	<1.5±0.64	<1.5±0.64	<1.5±0.64
$[SiII]$34.8μm	Long-High	3.5±0.9	23.7±5.7	7.9±1.9

[a]Assumed distribution over scale of Long-Hi module (see text)

[b]ine may be marginally detected.